

# Probabilistic slope stability assessment of dikes along the Lek river in the Netherlands

Tuan Dobar Yos Firdaus Simanjuntak

Het Hoogheemraadschap De Stichtse Rijnlanden, Houten, The Netherlands, [yos.simanjuntak@hdsr.nl](mailto:yos.simanjuntak@hdsr.nl)

Cor Bisschop

Greenrivers BV, Elburg, The Netherlands

**ABSTRACT:** This paper presents a procedure, under a probabilistic framework, for assessing the safety of river dikes against inner slope failure, known as macro-instability. The assessment is applied to a specific dike cross-section between Jaarsveld and Klaphek in the province of Utrecht, the Netherlands. For given external water levels, conditional failure probabilities, referred to as fragility points, are determined using the Monte Carlo Importance Sampling (MCIS) method implemented in the limit equilibrium model D-Stability. These fragility points, together with the fragility curve for wave overtopping, are used to derive a weighted fragility curve that accounts for the influence of wave overtopping under extreme hydraulic conditions. The total annual failure probability, or overall reliability index, is then obtained by integrating the weighted fragility curve over the probability density function of the water level. The safety of the dike against macro-instability at the cross-section level is subsequently evaluated by comparing the overall reliability index with the target value. The results presented in this paper indicate that the proposed methodology is effective for inner slope reliability analyses, as it allows for the estimation of the total annual failure probability using spreadsheets and accessible geotechnical software, such as D-Stability. For the purpose of validation, the results are compared with those obtained using the Probabilistic Toolkit.

**KEYWORDS:** Macro-stability, river dike, fragility curve, reliability analysis.

## 1. INTRODUCTION

Since the introduction of the new Dutch safety standards and guidelines in 2017, the assessment of primary dikes has been based on acceptable probabilities of flooding rather than the exceedance frequencies of hydraulic loads. As of 2021, over 1,600 kilometres of river dikes in the Netherlands have been identified as requiring reinforcement, as their estimated failure probabilities exceed the acceptable threshold (HWBP, 2020).

To maintain flood protection and ensure compliance with the new standards, the 55-kilometre Lekdijk, extending from Amerongen to Schoonhoven and protecting a large part of central and western Netherlands, is now undergoing extensive evaluation and reinforcement. The water authority HDSR (Het Hoogheemraadschap De Stichtse Rijnlanden) coordinates this project under the programme name Sterke Lekdijk.

One of the primary failure mechanisms affecting dikes is the sliding of the inner slope, known as macro-instability. This failure mode may develop during periods of high water levels, when pore water pressure within and beneath the dike body increases, thereby reducing effective stress and soil shear strength. Once inner slope instability occurs, the dike may sustain damage to such an extent that it can no longer withstand floodwater levels. Under high water levels combined with wave action, overtopping and slope instabilities can ultimately lead to a dike breach.

The saturated condition of the dike induced by overtopping is another crucial factor that can trigger its macro-instability. To explore the interaction between overtopping and water levels under extreme conditions, we consider two scenarios in this study: (a) the absence of infiltration due to overtopping, and (b) the complete infiltration due to overtopping.

Since geotechnical parameters are inherently uncertain due to measurement errors and statistical uncertainty, traditional factors of safety based on deterministic slope stability analyses have increasingly been replaced by reliability-based slope analyses. Recent Dutch dike reinforcement projects (e.g., De Koning et al., 2018; Simanjuntak et al., 2019) have applied reliability analyses for macro-stability, often employing the First Order Reliability Method (FORM) introduced by Hasofer and Lind (1974), which is widely recognised for its robust performance and computational efficiency.

The implementation of FORM, however, requires great care, as it relies on a priori assumptions regarding the shape of the governing slip surface. In this method, the slip surface is assumed to be identical to that associated with the minimum factor of safety obtained from semi-probabilistic analyses, called the deterministic critical slip surface, which does not necessarily correspond to the governing slip surface in probabilistic analyses. Performing sensitivity analyses, which are often a time-consuming process, is therefore essential when applying FORM in order to ensure an accurate estimation of the probability of failure.

In this study, we identify the governing slip surface using the Monte Carlo Importance Sampling (MCIS) method (Van der Meer et al., 2022), which is an adaptive variant of the crude Monte Carlo approach. Using the MCIS method, we are able to select a limited number of potential slip surfaces from among a large number of slip surfaces. Moreover, this method allows the slip surface to evolve freely without predefined assumptions, resulting in a more accurate representation of the slip surface in probabilistic slope analyses. Once the governing slip surface has been identified, a fragility point that defines the probability of failure conditional on the external water level can be established, which serves as a basis for constructing a fragility curve.



Figure 1. Dike segment between Jaarsveld and Klaphek.

Table 1. Random variables

Soil	Volumetric Weight $\gamma_{sat}/\gamma_{unsat}$ [kN/m <sup>3</sup> ]	Undrained Shear Strength Ratio $S$ [-]	Strength Increase Exponent $m$ [-]	Pre-Overburden Pressure $POP$ [kPa]	Critical State Friction Angle $\phi'_{cs}$ [°]
Dike Clay	18.9/18.9				$\mu$ 31.98, $\sigma$ 0.91
Silty Clay	16.1/16.1	$\mu$ 0.32, $\sigma$ 0.02	$\mu$ 0.94, $\sigma$ 0.01	$\mu$ 32.40, $\sigma$ 11.75	$\mu$ 37.54, $\sigma$ 2.55
Clay Organic	13.2/13.2	$\mu$ 0.27, $\sigma$ 0.02	$\mu$ 0.79, $\sigma$ 0.04	$\mu$ 40.70, $\sigma$ 21.50	
Peat Clayey	11.3/11.3	$\mu$ 0.38, $\sigma$ 0.03	$\mu$ 0.55, $\sigma$ 0.02	$\mu$ 43.20, $\sigma$ 17.85	
Peat	10.4/10.4	$\mu$ 0.38, $\sigma$ 0.03	$\mu$ 0.55, $\sigma$ 0.02	$\mu$ 43.20, $\sigma$ 17.85	
Sand Pleistocene*	20.0/18.0				$\mu$ 34.00, $\sigma$ 1.00

\* adopted from Rijkswaterstaat (2021)

Using the site-specific fragility curve for overtopping and the fragility points for both scenarios, we calculate the weighted failure probability for each water level. The failure probability for each external water level is then obtained by multiplying the weighted failure probability by the probability density function of the external water level. The total failure probability can subsequently be derived by computing the weighted sum of the failure probabilities across all external water levels.

First, this paper describes the essential data required to conduct reliability analyses for macro-stability, such as soil properties, water levels, and wave overtopping. Subsequently, it presents an approach for deriving a weighted fragility curve to account for the effects of wave overtopping. This is followed by a detailed, step-by-step calculation procedure for estimating the overall reliability index. Finally, the proposed methodology is applied to a representative dike cross-section located between Jaarsveld and Klaphek as depicted in Figure 1, the dike segment of which also belongs to the broader Sterke Lekdijk.

## 2. MODELLING UNCERTAINTIES IN SOIL PARAMETERS AND HYDRAULIC LOADS

### 2.1 Soil parameters and pre-overburden pressure

In accordance with the Dutch statutory safety assessment, dike resistance to macro-instability must be evaluated under the Critical State Soil Mechanics (CSSM) framework, as described by Schofield and Wroth (1968). Within this framework, the shear strength for drained soils is calculated using the critical state friction angle  $\phi'_{cs}$ . For undrained soils, the shear strength is modelled according to the Stress History and Normalized Soil Engineering Properties (SHANSEP) formulation (Ladd and Foott, 1974), which incorporates both the stress history and the stress path of the soil.

$$s_u = \sigma'_v S (OCR)^m \quad (1)$$

where  $S$  denotes the undrained shear strength ratio for normally consolidated soil,  $m$  is the strength increase exponent, and  $OCR$  is the over-consolidation ratio, defined as the ratio of the pre-consolidation stress  $\sigma'_p$  to the in-situ vertical effective stress  $\sigma'_v$ , and  $POP$  refers to the pre-overburden pressure, such that  $\sigma'_p = \sigma'_v + POP$ .

Between Jaarsveld and Klaphek, a total of 74 CAU triaxial tests, 34 DSS tests, 52 oedometer tests, and 20 CRS tests were performed on samples collected from various locations along the dike segment, forming a regional dataset. The  $S$  and  $m$  parameters for clay were derived from the triaxial tests at a strain level of 25%, whereas for peat they were obtained from the DSS tests at a strain level of 40% (Rijkswaterstaat, 2021).

For each undrained soil type within the same geological deposit, we estimate the mean values  $\mu S$  and  $\mu m$  simultaneously using linear regression between  $s_u/\sigma'_v$  and  $OCR$ . The mean critical state friction angle  $\mu\phi'_{cs}$  is determined based on the tangency points of the Mohr circles. Further details on the soil parameter estimation can be found in Rijnveld and Lengkeek (2025).

To determine the mean pre-overburden pressure  $\mu POP$  for peat and clay, we apply a shifted lognormal distribution fitted using the method of moments as described by Van der Krogt (2023), which accounts for statistical uncertainty. The random variables for soil parameters and pre-overburden pressure used in this study are presented in Table 1. For the sand aquifer, we adopt the data from the literature (Rijkswaterstaat, 2021).

### 2.2 Hydraulics loads

#### 2.2.1 External water levels

The external water levels at the location of the cross-section are governed by river discharge, tidal intrusion, and wind-driven waves. In this study, the water level data were obtained using the numerical model Hydra-NL, which computes water levels only at a selected set of fixed output locations. Therefore, we selected the location closest to the dike cross-section used in the semi-probabilistic analysis to derive the relevant water levels.

We account for land subsidence over a 50-year period by applying a surcharge to the external water level, in accordance with the Dutch guidelines that require an assessment of whether the dike meets legal safety standards over at least the next 50 years. The corresponding data are provided in Table 2. We use the frequency curve as the probability distribution for the water level and subsequently fit a Gumbel distribution to these data, as shown in Figure 2.

Table 2. Exceedance probabilities of water level

Return Period [Years]	Frequency [Year <sup>-1</sup> ]	Water Level [m NAP*]
10	0.10000	+4.97
30	0.03333	+5.56
100	0.01000	+5.96
300	0.00333	+6.19
1,000	0.00100	+6.37
3,000	0.00033	+6.49
10,000	0.00010	+6.60
30,000	0.00003	+6.69
100,000	0.00001	+6.80

\* NAP is vertical datum (in Dutch: Normaal Amsterdams Peil)

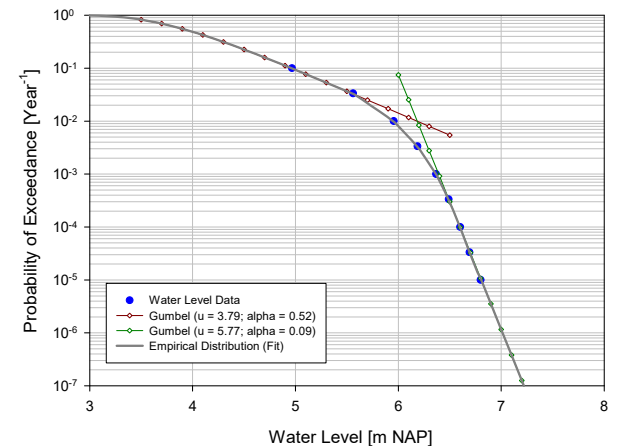


Figure 2. Fitted Gumbel distribution to water level data.

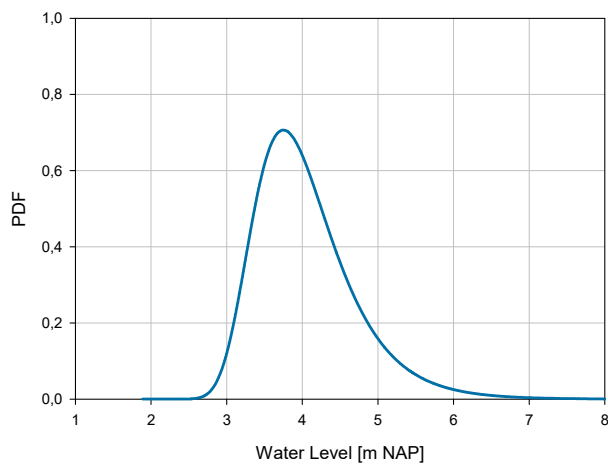


Figure 3. Probability density function of water level.

The floodwater level is defined as the water level with a frequency equal to the acceptable probability of flooding. It is the water level with an exceedance probability of 1/10,000 per year, which, at the cross-section location, corresponds to NAP +6.60 m. We also derive the probability distribution of external water level in the form of a probability density function, as illustrated in Figure 3. These data are required as input for conducting reliability analyses using the Probabilistic Toolkit.

### 2.2.2 Polder water level

The groundwater level in the protected area, also known as the polder water level, is typically regulated, resulting in limited fluctuations. At the cross-section location, it is maintained at NAP +0.07 m. Given the limited fluctuations, we consider the uncertainty in the polder water level to be negligible.

### 2.2.3 Hydraulic head

The hydraulic head in the sand aquifer under daily water level conditions can be determined based on measurements collected from monitoring wells. Under high water level conditions, we estimate the design value of the hydraulic head using analytical formulae for steady-state flow, as described in TAW (2004).

### 2.2.4 Intrusion zone

During high water levels, an increased hydraulic head in the sand aquifer causes vertical intrusion into the overlying clay or peat aquitard. This phenomenon can result in an increase in pore water pressure, and thus a reduction in both effective stress and soil shear strength.

The thickness of the vertical intrusion, also known as the intrusion zone, is governed by soil permeability and the phreatic level. This zone increases as the duration of high water levels lengthens (TAW, 2004). Owing to the lack of site-specific data, we adopt a conservative estimate of 3 metres for the intrusion zone in this study.

### 2.2.5 Infiltration due to wave overtopping

The combination of high water levels and wind can result in wave overtopping. Water can infiltrate into the dike and raise the phreatic line. The extent to which overtopping leads to full saturation of the dike remains uncertain, because it depends on several factors, such as the permeability of the cover layer.

In this study, we assume full saturation of the dike when overtopping begins at a discharge of 0.001 m<sup>3</sup>/s/m or 1 l/s/m. Accordingly, we consider two scenarios: (1) the absence of infiltration due to overtopping, and (2) the complete infiltration due to overtopping. The following assumptions are applied for the schematisation of pore water pressure:

- in the absence of infiltration, we schematise the phreatic line in the dike body under steady-state conditions, in accordance with TAW (2004).
- in the case of complete infiltration, we assume the dike is fully saturated, with a hydrostatic distribution of pore water pressure with depth.

To gain insight into the interaction between overtopping and external water levels under extreme conditions, a fragility curve for wave overtopping is required. Figure 4 illustrates the conditional probability of failure due to wave overtopping at the cross-section location (Pleiter and Duits, 2023). This curve expresses the probability of failure due to wave overtopping as a function of the external water level, and is used to derive the weighted conditional failure probability for each water level. This means that we first calculate the fragility points for both scenarios, and then weight them for each external water level by incorporating the fragility curve for wave overtopping.

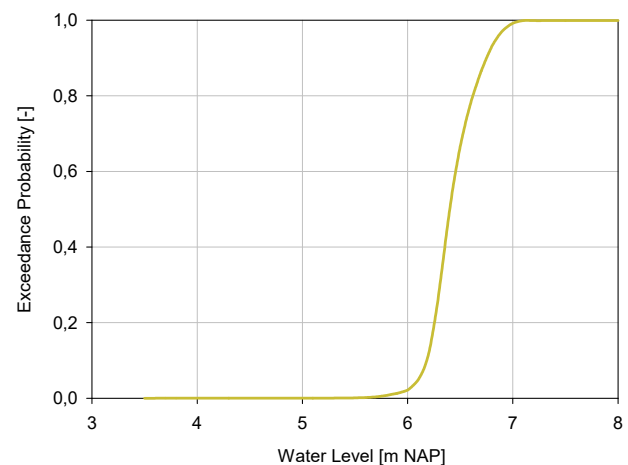


Figure 4. Fragility curve for wave overtopping at the cross-section location for an overtopping discharge of 1 l/s/m.

## 2.3 Traffic load

Between Jaarsveld and Klaphek, a road runs along the dike crest. In this study, we consider the traffic load acting on the dike, as it may influence the overall macro-stability of the dike.

In the reliability assessment of dikes in the Netherlands, the traffic load has so far been treated as a point estimate due to the limited availability of statistical data. Nevertheless, the likelihood of an extreme traffic load occurring simultaneously with extreme water levels is low, particularly when overtopping occurs and traffic management measures are put in place during high water events.

Under normal conditions, or when water levels correspond to an annual exceedance probability of up to 1/50, a maximum traffic load of 15 kPa is permitted on the dike. During dike inspection or restoration work, and under water levels with an exceedance probability of up to 1/1,000 per year, the traffic load is restricted to 8 kPa. At higher water levels corresponding to an annual exceedance probability of less than 1/1,000, no traffic load is allowed on the dike crest (HDSR, 2022).

In D-Stability, we schematise the traffic load over a width of 2.5 metres, measured from the inner crest. We assume a load dispersion angle of 30 degrees, with a consolidation degree of 0% for cohesive layers and 100% for non-cohesive layers. We adopt a point estimate approach for the traffic load by using its corresponding design value for each external water level.

In the scenario of complete infiltration or when the dike is assumed to be fully saturated, no traffic load schematised in the model, in accordance with the project-specific design principles (HDSR, 2022).

## 2.4 Model uncertainty

In general, the shape of the slip surface is non-circular. In order to account for non-circular slip surfaces under plane strain conditions, we employ the Uplift-Van model (Van, 2001).

Due to its simplified representation of physical processes, this model entails inherent uncertainty. In this study, we treat the model factor  $m_d$  for Uplift-Van as a lognormally distributed stochastic variable, with a mean  $\mu_{m_d}$  of 1.005 and a standard deviation  $\sigma_{m_d}$  of 0.033, according to Van Duinen (2015).

## 3. TARGET RELIABILITY INDEX

The dike between Jaarsveld and Klaphek, with a total length of 23 kilometres, is by law required to meet a failure probability requirement for macro-stability at the cross-section level  $P_T$  of  $2.47 \times 10^{-7}$  per year, corresponding to a target reliability index  $\beta_T$  of 5.03. This safety requirement is derived using the following equation (Rijkswaterstaat, 2021):

$$P_T = \frac{\omega P_{norm}}{1 + \left(\frac{aL}{b}\right)} \quad (2)$$

where  $P_{norm}$  is the maximum acceptable failure probability of a dike segment,  $\omega$  corresponds to the failure probability factor for macro-stability,  $L$  indicates the total length of the dike segment,  $a$  represents the fraction of the dike segment length that is sensitive to macro-stability, and  $b$  is the length of independent, equivalent dike sections for macro-stability.

For the relationship between the target reliability index and the required factor of safety in semi-probabilistic calculations, readers are referred to Kanning et al. (2017).

## 4. ADOPTED METHODOLOGY

A fragility curve, which represents the conditional probability of failure (or equivalently, the conditional reliability index) as a function of the external water level, can be constructed using a limited number of fragility points through linear interpolation. In the Netherlands, this curve is typically presented as a  $\beta$ - $h$  curve. For macro-stability assessments, this curve is commonly constructed for two scenarios: (1) an unsaturated dike without infiltration, and (2) a saturated dike with infiltration as a result of wave overtopping.

Based on the fragility curve for wave overtopping, we compute a weighted conditional failure probability, using the following equation:

$$P(F|h) = P(F|h_{infiltration}) \times P(q_{overtopping}|h) + P(F|h_{no-infiltration}) \times [1 - P(q_{overtopping}|h)] \quad (3)$$

where  $P(F|h)$  denotes the probability of failure conditional on a water level  $h$ ,  $P(F|h_{infiltration})$  is the probability of failure with infiltration conditional on a water level  $h$ ,  $P(F|h_{no-infiltration})$  is the probability of failure without infiltration conditional on a water level  $h$ , and  $P(q_{overtopping}|h)$  is the probability of overtopping given a water level,  $h$ .

The total probability of failure is obtained by integrating the failure probability  $P(F|h)$  over the probability distribution of water level  $f_h$ .

$$P(F) = \int P(F|h) f_h(h) dh \quad (4)$$

Or in terms of the reliability index, it can be expressed as:

$$P(F) = \int \Phi[-\beta(h)] f_h(h) dh \quad (5)$$

Using spreadsheets, this integration can be performed by multiplying the conditional failure probabilities at each water level by the probability density function of the water level. Subsequently, the design point for the water level, defined as the water level associated with the highest failure probability, can be identified.

In the following, we describe a step-by-step procedure to estimate the overall reliability index of river dikes with regard to macro-stability:

- A. Define the required input data, including soil parameters, water levels, and wave overtopping together with their associated statistical properties;
- B. Configure the deterministic macro-stability analysis model in the limit equilibrium model D-Stability. Compute the factor of safety associated with the floodwater level, which is defined in this study as the water level corresponding to an exceedance probability of 1/10,000 per year. The factor of safety and the deterministic critical slip surface form the basis for the probabilistic computations;
- C. Based on the mean values of the soil properties, perform probabilistic computations by means of the MCIS method to identify the probabilistic slip surface and to estimate the conditional reliability index. When desired, retain the slip surface identified by the MCIS method and re-run the probabilistic computations by using the FORM to evaluate the reliability index. This additional step aims to improve the accuracy of the conditional reliability index beyond the initial MCIS-based estimation;
- D. Repeat steps B and C for each external water level, and perform the MCIS simulations for both scenarios: the first scenario representing an unsaturated dike, and the second a fully saturated dike. Identify all relevant fragility points for both scenarios. This step generates two distinct sets of fragility points;
- E. Using the fragility curve for wave overtopping as depicted in Figure 4, determine the probability of failure due to wave overtopping for each water level. Then, together with the conditional fragility points obtained in step D, derive the weighted conditional failure probability for each water level by applying Equation (3). This step results in a single, weighted fragility curve;
- F. Combine the weighted fragility curve obtained in step E with the probability density function of the external water level, as presented in Figure 3. The total failure probability can then be obtained by solving Equation (4), which is the weighted summation of failure probabilities for each water level. This step also provides the overall reliability index;
- G. Based on the conditional probability of failure obtained in step F, identify the design point for the external water level, that is, the water level that corresponds to the maximum probability of failure.
- H. Optionally, validate the results obtained in steps F and G by comparing them with those obtained using a more advanced probabilistic model, such as the Probabilistic Toolkit. In the Probabilistic Toolkit, the reliability analyses require the fragility curve derived in step E, as well as the probability density function of the water level as inputs.

## 5. CASE STUDY

### 5.1 Geometry

The study examines a clay dike with an inner slope inclined at a vertical-to-horizontal ratio (V:H) of 1:4.8. The projected crest elevation for the next 50 years is NAP +7.4 m. The cover layer beneath the dike is approximately 9.6 m thick and consists of compressible soil layers, primarily clay and peat.

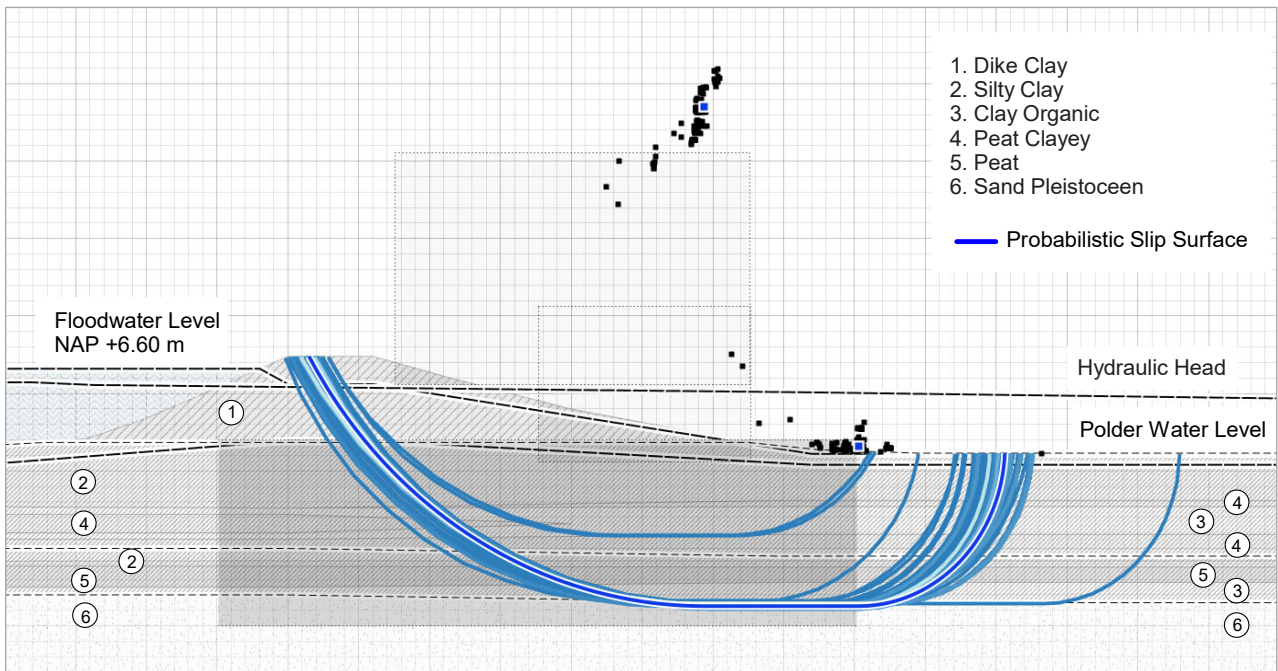


Figure 5. Cross-section profile and the governing slip surface identified using MCIS for the floodwater level and without infiltration.

Table 3. Results of conditional reliability index for both scenarios

Return Period [Years]	Water Level $h$ [m NAP]	Scenario Without Infiltration			Scenario With Infiltration		
		Factor of Safety $SF$ [-]	Reliability Index $\beta$ [-]	Slip Surface <sup>c</sup> [m NAP]	Factor of Safety $SF$ [-]	Reliability Index $\beta$ [-]	Slip Surface <sup>c</sup> [m NAP]
10	+4.97	1.23	6.89	-8.37	1.19	5.63	-4.13
30	+5.56	1.18	6.50	-8.62	1.15	5.63	-4.13
50	+5.80	1.16	6.15	-8.68	1.13	5.60	-4.13
1,000	+6.37	1.11	5.38	-8.64	1.08	4.90	-8.65
10,000	+6.60 <sup>a</sup>	1.09	5.14	-8.67	1.05	4.45	-8.67
100,000	+6.80	1.07	4.74	-8.70	1.04	4.14	-8.79
300,000	+6.90 <sup>b</sup>	1.06	4.53	-8.74	1.03	4.00	-8.72

<sup>a</sup> the floodwater level associated with the annual exceedance probability of 1/10,000 (in Dutch: WBN)

<sup>b</sup> WBN + 30 cm

<sup>c</sup> probabilistic slip surface

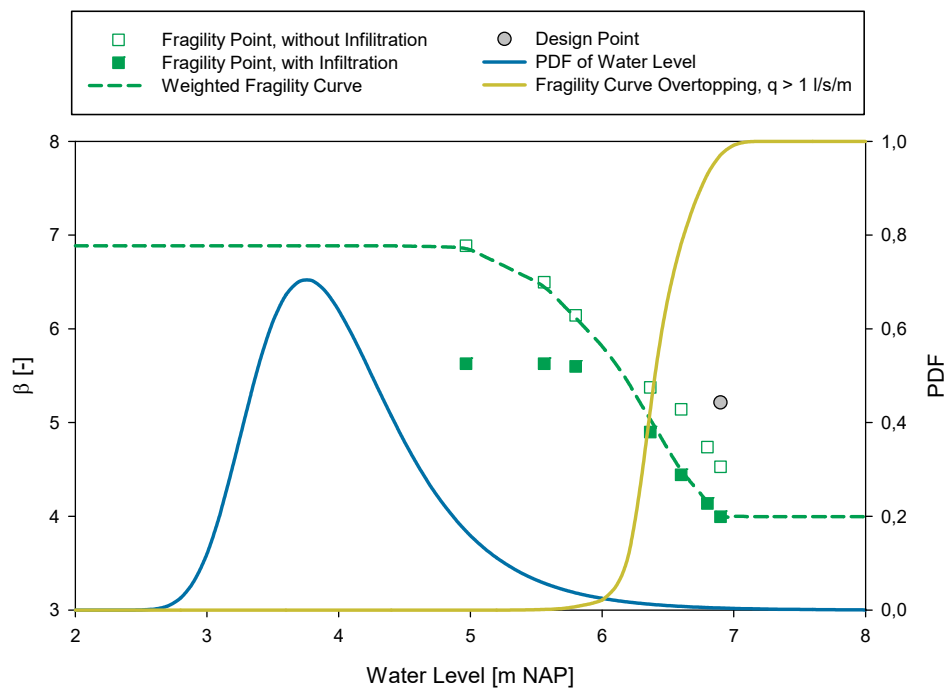


Figure 6. Fragility curves and probability density function of water level.

The bottom of the cover layer at the hinterland lies at NAP -8.5 m. The average daily river water level is approximately NAP +0.45 m. Under daily conditions, the phreatic surface in the dike body reaches an elevation of NAP +1.95 m. The polder water level is maintained at NAP +0.07 m. Figure 5 presents the cross-sectional profile of the dike analysed in this study.

## 5.2 Correlations

In this study, we derived the undrained soil parameters  $S$  and  $m$  for each soil type simultaneously using linear regression. Consequently, these parameters are considered to be fully correlated within each individual soil layer.

Because the available laboratory test results do not specify differences in soil properties beneath and adjacent to the dike, we apply, for a given soil type, the same probability distribution for the  $POP$  to both locations. However, we treat the  $POP$  beneath and adjacent to the dike as uncorrelated, since the stress histories differ between these locations.

## 6. RESULTS OF RELIABILITY ANALYSES

The factor of safety associated with an annual exceedance probability of 1/10,000, corresponding to the floodwater level of NAP +6.60 m, is 1.09. The bottom level of probabilistic slip surface corresponding to each water level is given in Table 3.

Figure 6 shows the weighted fragility curve, the probability density function of external water level, and the design point, illustrating their interaction and combined influence on the total failure probability, which in the Netherlands is also commonly expressed in terms of reliability index. The analysis yields an overall reliability index  $\beta$  of 5.22, corresponding to a total failure probability of  $9.17 \times 10^{-8}$  per year.

Furthermore, we identify the design point for the external water level as NAP +6.90 m. This water level corresponds to the water level corresponds to the point at which the product of the weighted fragility curve and the probability density of the external water level reaches its maximum, thereby contributing most significantly to the total failure probability.

Table 4 presents the overall reliability index and the design point for the external water level obtained using the proposed methodology. The results show good agreement with those obtained using the Probabilistic Toolkit, indicating consistency between the two approaches. Since the calculated reliability indices exceed the target value  $\beta_r$  of 5.03, the macro-stability of the dike at the cross-section level is considered satisfactory.

Table 4. Results of reliability analyses

Instruments [-]	Reliability Index $\beta$ [-]	Design Point $h$ [m NAP]
D-Stability + Spreadsheet	5.22	+6.90
D-Stability + Prob. Toolkit	5.20	+6.90

## 7. CONCLUDING REMARKS

This study presents a methodology for conducting reliability analyses of macro-stability, demonstrated through a case study of a dike cross-section situated between Jaarsveld and Klaphek in the province of Utrecht, the Netherlands.

The analyses demonstrate that the MCIS method provides an effective approach for identifying the governing slip surface. In addition, the MCIS method facilitates the efficient estimation of the reliability index. Once fragility points are determined, they can serve as a basis for constructing a fragility curve.

To assess the impact of wave overtopping under high water level conditions, two scenarios were considered: an unsaturated dike without infiltration, and a saturated dike with infiltration. These scenarios yielded two distinct sets of fragility points.

Using the site-specific fragility curve for wave overtopping and the fragility points obtained for both scenarios, a weighted failure probability for each water level can be calculated in a spreadsheet. The failure probability for each water level can be obtained by multiplying the weighted failure probability by the probability density function of the external water level. The overall reliability index can then be determined by computing the weighted sum of the failure probabilities for each external water level.

The results indicate that the proposed methodology is not only effective for slope reliability analyses, but also well suited for broader practical applications, since it allows for estimating the overall reliability index with a spreadsheet and accessible geotechnical software, such as D-Stability.

When schematising pore water pressure across stratified soil layers, two random variables require careful consideration: the assumed depth of hydrostatic pressure and the extent of the intrusion zone above the sand aquifer. In this study, both were conservatively modelled in D-Stability. This approach, while conservative, does not compromise the validity of the dike assessment against macro-instability. If needed, the influence of these variables on the overall reliability index can be further assessed through discrete scenario analyses.

## 8. REFERENCES

- De Koning, M., Goeman, D.G., Bisschop, C., Boxhoorn, L., and Weijland, M. 2018. Probabilistische Analyse van Waarde bij Dijkversterkingsproject. *Land & Water*, Vol.5, 24-26 (in Dutch).
- D-Stability. 2025. *Slope Stability Software for Soft Soil Engineering - User Manual*. Version 2025.01. Deltares.
- Hasofer, A. and Lind, N. 1974. Exact and Invariant Second-Moment Code Format. *Journal of the Engineering Mechanics Division*, 100(1), 111-121.
- HDSR. 2022. *Strategische Nota van Uitgangspunten* (in Dutch).
- HWBP. 2020. *Projectenboek HWBP 2021*.
- Kanning, W., Teixeira, A., van der Krogt, M., and Rippi, K. 2017. *Derivation of the Semi-Probabilistic Safety Assessment Rule for Inner Slope Stability*. Deltares Report 1230086-009-GEO-0030.
- Ladd, C.C. and Foot, R. 1974. New Design Procedure for Stability of Soft Clays. *Journal of Geotechnical Engineering Division*, 100(7), 763-786.
- Pleiter, G. and Duits, M. 2023. *Fragility Curves bij Zes Dijkpalen op het Traject Jaarsveld-Klaphek*. HKV-Lijn in Water PR4643.20 (in Dutch).
- Probabilistic Toolkit. 2025. *User Manual*. Version 2025.3.4. Deltares.
- Rijkswaterstaat. 2021. *Schematiseringshandleiding Macrostabiteit WBI2017*. Versie 4.0 (in Dutch).
- Rijneveld, B. and Lengkeek, A. 2025. *Memo Spreadsheets voor Parameterbepaling*. De Innovatieversneller (DIV) (in Dutch).
- Simanjuntak, T.D.Y.F., Bakker, H.L., Goeman, D.G., Haasnoot, J.K. and Bisschop, C. 2019. Macro-Stability Assessment of Dikes Using Two Different Probabilistic Models. *Proc. 17<sup>th</sup> European Conference on Soil Mechanics and Geotechnical Engineering (ECSMGE)*, Reykjavik.
- Schofield, A.N. and Wroth, C.P. 1968. *Critical State Soil Mechanics*. McGraw-Hill.
- TAW. 2004. *Technisch Rapport Waterspanningen bij Dijken (TRWD)*. Technische Adviescommissie Waterkeringen (in Dutch).
- Van der Krogt M. 2023. *Handreiking Faalkansanalyse Macrostabiteit Actuele Sterkte*. Deltares (in Dutch).
- Van der Meer, A., Brinkman, R. and Kanning, W. 2022. Probabilistic Slope Stability Assessment with Adaptive Monte Carlo Importance Sampling. *Proc. 8th International Symposium on Geotechnical Safety and Risk (ISGSR)*, Newcastle, 434-439.
- Van Duinen, A. 2015. *Modelonzekerheidsfactoren Spencer-Van der Meij Model en Ongedraineerde Schuifsterkte*. Deltares (in Dutch).
- Van, M.A. 2001. New Approach for Uplift Induced Slope Failure. *Proc. 15th International Conference on Soil Mechanics & Geotechnical Engineering (ICSMGE)*, Istanbul, 2285-2288.